RSC Advances

RSC Advances

www.rsc.org/advances

ROYAL SOCIETY OF CHEMISTRY

www.rsc.org/advances
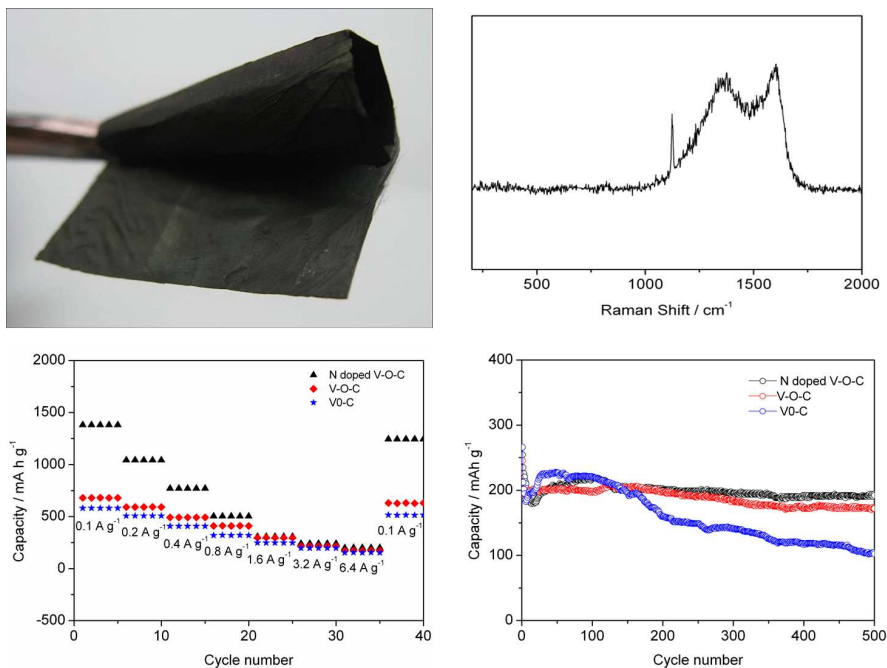
Highly flexible vanadium and nitrogen co-doped carbon films were synthesized by electrospinning, delivering an outstanding discharge capacitance of 1380 mAh g^{-1} at 0.1 A g^{-1}. The Coulombic efficiency was as high as 63.3% and a capacity retention ratio of 80% was obtained after cycling at 6.4 A g^{-1} for 500 times.

.

ARTICLE TYPE

Free-standing nitrogen doped V-O-C nanofiber film as promising electrode for flexible lithium-ion batteries

Xia Chen[a,b], Yujing Sha[a,b], Rui Cai[a,b], Moses O. Tade´[c], Zongping Shao[a,c,d]

Flexible vanadium and nitrogen co-modified amorphous carbon nonwoven films are successfully
5 synthesized and applied as free-standing film anodes for lithium-ion batteries (LIBs). The developed films exhibit outstanding capacity with an initial Coulombic efficiency of 63.3%. Furthermore, favorable rate capability and good cycling stability are achieved. Cycling at a current density of 0.1 A g^{-1}, the specific capacity of the nitrogen doped V-O-C nanofiber film reaches as high as 1380 mAh g^{-1}, showing considerable promise for use as an electrode for flexible lithium-ion batteries.

Introduction

10 Lithium-ion batteries (LIBs) are the most frequently used power sources in personal electronics because of their advantageous features [1-4]. Recently, the development of flexible LIBs has also been the focus of increasing interest with the advances in
15 soft electronics [5-8]. The primary technical challenge for flexible LIBs is the electrodes. As the most used anode material in commercial LIBs, graphite, which is a layered structure oxide that stores charge through the reversible insertion/extraction of lithium into/from the lattice spaces of its constituent graphene
20 layers, has the disadvantages of low capacity, poor rate performance and rigid mechanical properties. In addition, state-of-the-art electrodes for LIBs, which are usually composed of an active material, conductive additive and binder, should be deposited over metallic foil current collectors. The use of
25 additives reduces the overall energy density of LIBs but introduces potential side reactions. The deposition of electrode materials onto the metallic foils may also introduce large internal stresses inside the cell during the cycling process because the current collector, which has fixed dimensions, can not
30 accommodate the volumetric change of the electrode materials. Due to the above considerations, self-supported additive-free film electrodes with superior mechanical flexibility and high energy/power density are highly attractive for flexible LIBs. Carbon has many allotropes and morphologies, and different
35 types of carbons may have different lithium storage mechanisms and capabilities. Of the many types of carbon materials, nano-structured porous carbon is of particular interest as an electrode material for LIBs with high lithium storage capability. The nanostructure can significantly reduce the lithium diffusion
40 distance, whereas the rich pores will greatly increase the area of the liquid electrolyte-electrode (carbon) interface [4]. In addition, the carbon can be doped with foreign elements, such as N and B, to provide further improvement in electric and/or electrochemical performance. We have previously demonstrated that vanadium
45 doping increased the specific surface area of amorphous carbon

nanofibers, thereby improving the electrochemical performance of the carbon as a supercapacitor anode with an aqueous electrolyte. On the other hand, it is well known that nitrogen doping can increase the electrical conductivity and alter the
50 electronic structure of carbon [9,10], which suggests that co-doping with vanadium and nitrogen may further improve the electrochemical performance of amorphous carbon.

In this communication, we report the successful fabrication and application of a flexible V and N co-modified amorphous carbon
55 nonwoven film as a free-standing film anode for LIBs with an organic liquid electrolyte. Outstanding performance with a reversible capacity of up to 1380 mAh g^{-1} at a current density of 0.1 A g^{-1}, attractive rate capability, and fairly good cycling stability were obtained. These films thus have considerable
60 potential for practical application as novel electrode materials in flexible LIBs.

Experimental

A two-step calcination was employed for the synthesis of N doped V-O-C nonwoven films. First, 0.4 g polyvinylpyrrolidone
65 (PVP) and 0.4 g polyacrylonitrile (PAN) were dissolved in 4.5 ml dimethylformamide (DMF) with consistent stirring for 2 h. Afterwards, 0.08 g vanadyl acetylacetone (VO(acac)$_2$) was added. Finally the green nonwoven films were prepared by electrospinning using above vanadium-containing organic
70 solution precursor [11], which was first calcined in an argon atmosphere at 800 °C for 1 h and then in an ammonia atmosphere at 600 °C for an additional 2 h. The as-obtained sample was named N doped V-O-C. For comparison, carbon films without VO(acac)$_2$ in the precursor were also prepared in a similar
75 manner and named V0-C. The V-containing nonwoven film that was calcined only in Ar was named V-O-C.

Material characterization

The crystalline structure was examined by X-ray diffraction (XRD) using a Bruker D8 Advance diffractometer equipped with filtered Cu Kα radiation at room temperature. Raman spectra were recorded on a HR800 UV Raman microspectrometer 5 (JOBIN YVON, France) with an argon laser (λ=514.53 nm) excitation source. Field-emission scanning electron microscopy (FE-SEM, Hitachi S-4800) was used to observe the sample morphologies. The V content in the film was analyzed by Thermo-gravimetric analysis (TGA) on a NETZSCH STA 449 10 with the test temperature ranging from 30 to 800 °C under air atmosphere, and with a heating rate of 10 °C min^{-1}.; meanwhile, the N content was characterized by elemental analysis using Vario Elcube CHONS (Element ar Analy sensyteme GmbH, Germany). The electrochemical performance of the electrode was 15 measured with 2016 coin cells. Li metal was used as the anode, 1 mol L^{-1} LiPF$_6$ in a mixture of ethylene carbonate (EC) and dimethyl carbonate (DMC) (1:1 by volume) was used as the electrolyte, and Celgard 2300 was used as the separator. The flexible film was used directly as the electrode without any binder 20 or conductive additive. The galvanostatic charge/discharge tests were conducted between 0.01-3.0 V vs. Li$^+$/Li on a NEWARE BTS computer-controlled galvanostat (Shenzhen, China).

Results and discussion

When the precursor film was subjected to the two-step 25 calcination, the nonwoven film morphology was well maintained. **Fig. 1a** presents the digital photographs of the as-prepared V0-C , V-O-C and N doped V-O-C nanofiber films. The films can still be easily folded and rolled up, which indicates that they all possess high mechanical flexibility. Typical SEM images of the 30 three samples are shown in **Fig. 1b**, which were formed through the random stacking of nanofibers with a diameter of approximately 300-400 nm. The morphology of modified N doped V-O-C samples were very similar to that of V0-C and V-O-C porous carbon nanofibers from the one-step calcination in an 35 argon atmosphere that we previously reported [**11**]. This result suggests that the second calcination in NH$_3$ after the formation of V-modified amorphous carbon did not have an obvious effect on the film morphology. However, the film considerably shrank and became extremely brittle when the green film was calcined 40 directly in ammonia, suggesting the importance of the two-step calcination for obtaining a flexible N doped V-O-C nanofiber film.

The XRD pattern of the N doped V-O-C nanofiber film is shown in **Fig. 2a**. This pattern reveals an amorphous structure with a 45 broad peak around 2θ of ~25 °. The Raman spectra in **Fig. 2b** exhibit the characteristic D and G vibration bands of carbon located at 1340 and 1594 cm^{-1}, respectively. The I$_D$/I$_G$ ratio was 1.17, suggesting that the carbon was amorphous. Compared to the V-O-C nanofiber film [**11**], another sharp vibrations peak at 50 approximately 1100 cm^{-1} appeared, which can be assigned to the T band originating from the sp^3 vibration of carbon[**12**, **13**]. Thus, the nitrogen was likely successfully doped into the carbon structure, which changed the molecular structure of carbon to induce the sp^3 vibration. Table 1 displays the element contents in 55 the films, which were analyzed by TGA and elemental analysis instruments. The specific contents of V and N in N doped V-O-C were determined to be 10.8 wt% and 9.48 wt%, respectively.
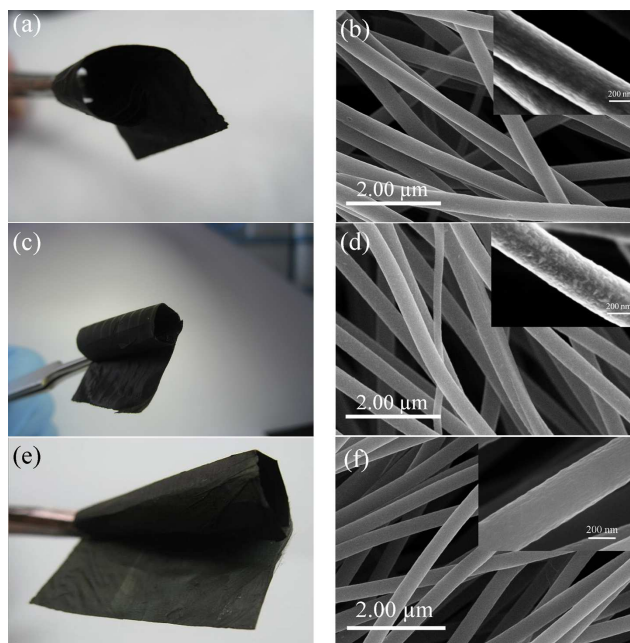

Fig. 1 Digital photos of the as-prepared (a) V0-C , (c)V-O-C and (e) N 60 doped V-O-C, and the corresponding SEM images of (b) V0-C , (d)V-O-C and (f) N doped V-O-C, respectively.
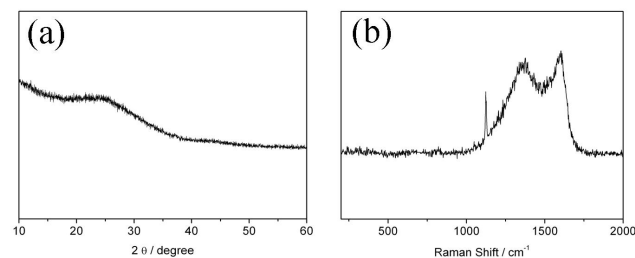

Fig. 2 (a) XRD pattern and (b) Raman spectra of the N doped V-O-C 65 nanofiber film.

Table 1. Specific element (C, H, N, V) contents in as-prepared nanofiber films.

Sample	C%	H%	N%	V%
V0-C	77.95	2.824	7.49	0
V-O-C	70.48	1.747	6.71	10.92
N doped V-O-C	66.44	1.649	9.48	10.80

To investigate the electrochemical performance of the as-70 fabricated nonwoven film as an anode for LIBs, half cells using the film as a free-standing electrode without any additive or binder, using lithium metal as the counter and reference electrodes, and using LiPF$_6$ as an organic liquid electrolyte were constructed. **Fig. 3a** shows the first and the second galvanostatic 75 discharge/charge curves within the potential range of 0.01-3.0 V at a current density of 0.1 A g^{-1}. During the first cycle, the voltage rapidly dropped and formed a plateau at approximately 0.8-1.0 V, which disappeared from the second cycle on. It was hypothesized that this plateau was related to the formation of a solid electrolyte 80 interface (SEI), which contributed largely to the irreversible capacity in first cycle [**14, 15**]. The first discharge and charge capacities reached values as high as 1201 and 760 mAh g^{-1},
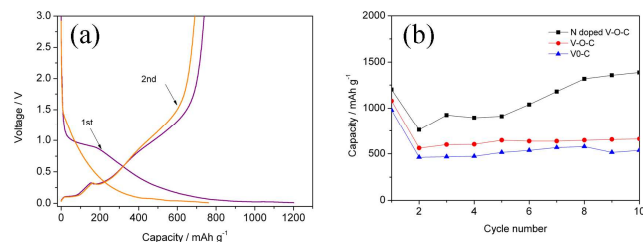
Fig. 3 (a) Charge and discharge curves of the N doped V-O-C nanofiber film at the current density of 0.1 A g^{-1}. (b) Cycling performances of the V0-C, V-O-C and N doped V-O-C nanofiber films, at the current density of 0.1 A g^{-1}.
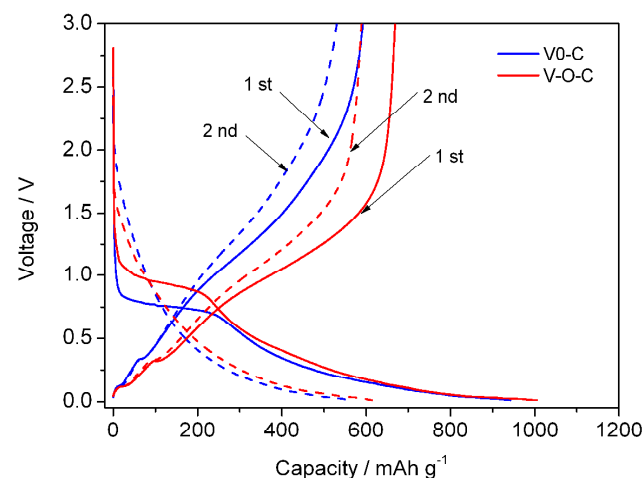

Fig. 4 Charge and discharge curves of the V0-C and V-O-C films at the current density of 0.1 A g^{-1}.
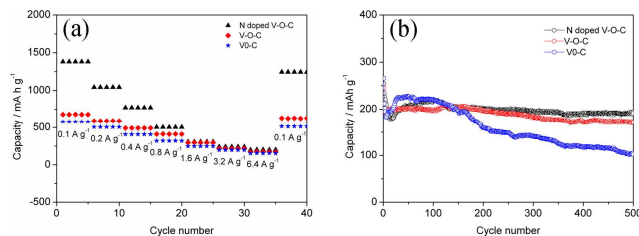

Fig. 5 (a) Specific capacitances of V0-C, V-O-C and N doped V-O-C nanofiber films at different current densities. (b) Corresponding cycling performances of V0-C, V-O-C and N doped V-O-C and V0-C samples at the current density of 6.4 A g^{-1}.
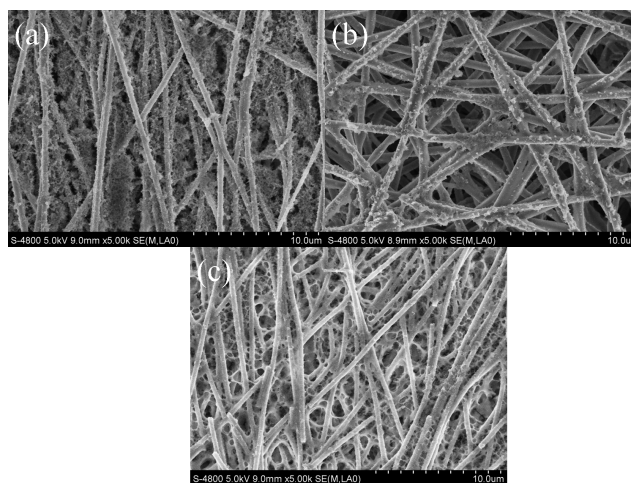

Fig. 6 SEM images of the (a) V0-C, (b) V-O-C and (c) N doped V-O-C nonwoven films after the galvanostatic discharge/charge cycling test at 6.4 A g^{-1} for 500 times.

respectively, indicating a first Coulombic efficiency of 63.3%; the Coulombic efficiency further increased to ~95% in the subsequent charge/discharge cycles. Huang et al. also prepared nitrogen-doped porous carbon nanofiber webs as anodes for LIBs using PPy nanofiber webs as the precursor [16]. A large irreversible capacity for the first cycle is of considerable importance for practical applications. Although Huang et al. achieved a rather high first discharge capacity of 2650 mAh g^{-1}, the Coulombic efficiency of the first cycle was only 48.3%. **Fig. 3b** shows the cycling performances of the V0-C, V-O-C and N doped V-O-C nanofiber film at a current density of 0.1 A g^{-1}. In the current study, a steady increase in discharge capacity with cycling time was observed from the third discharge/charge cycle on, and a discharge capacity as high as 1380 mAh g^{-1} was reached at the tenth cycle, which is comparable to the highest reversible capacity reported for carbon in the literature [17-19]. The improved performance may be explained by progressive wetting of the electrode material by the liquid electrolyte; consequently, partial electrode materials, which were initially unreachable by the electrolyte, became electrochemically active after the repeated cycling. For comparison, we also measured the capacities for amorphous carbon film prepared using the same electrospinning method (V0-C) and for the V-modified amorphous carbon film (V-O-C). As shown in **Fig. 4**, the second discharge capacities at a current density of 0.1 A g^{-1} were 564.0 and 614.8 mAh g^{-1} for the V0-C and V-O-C film electrodes, respectively, in comparison to 760 mAh g^{-1} for the N doped V-O-C nanofiber film electrodes. This result suggests that both the V

doping and the N doping improved the lithium storage capacity. It is known that the storage of lithium in carbon occurs through the adsorption of lithium at surface defects and through its reaction with surface oxygen-containing groups [20]. As demonstrated previously [11], the V doping increased the specific surface area of the carbon fibers, thereby providing more reaction sites. The N doping could increase the electric conductivity and the affinity of the electrodes to the liquid electrolyte. Consequently, improved electrode performance was realized through V and N co-doping. The rate capabilities of as-synthesized V0-C, V-O-C and N doped V-O-C nanofiber film electrode were further tested, and the results are shown in **Fig. 5a** (at each rate, the electrode was cycled 5 times to stabilize the capacity). For N doped V-O-C sample, the capacity reached 1380, 1042, 770, 502, 307, 240 and 200 mAh g^{-1} at current densities of 0.1, 0.2, 0.4, 0.8, 1.6, 3.2 and 6.4 A g^{-1}, respectively, suggesting good rate performance. After finishing the rate performance test at 6.4 A g^{-1}, the current was reduced again to 0.1 A g^{-1}, and a capacity of 1243 mAh g^{-1} was restored, which was approximately 90.1% of the initial capacity, suggesting that the electrode possesses good cycling stability. In comparison, V0-C and V-O-C samples demonstrated somewhat poorer rate capacities, as shown in **Fig. 5a**. To further demonstrate the cycling stability of the N doped V-O-C nanofiber film electrode prepared from the two-step calcination, a prolonged cycling test of 500 cycles was conducted at a high current density of 6.4 A g^{-1}. As shown in **Fig. 5b**, an initial capacity of 250 mAh g^{-1} was achieved, and it quickly decreased to 175 mA g^{-1} within the first

15 cycles. This process was likely related to the SEI formation. Then, a slow performance improvement was observed within the next approximately 100 cycles, which is likely due to the slow wetting of the electrode by the liquid electrolyte. After cycling for approximately 120 cycles, the capacity was stabilized. After 500 continuous discharge and charge cycles at 6.4 A g^{-1}, the capacity was maintained at 200 mAh g^{-1}. This result suggests that the as-prepared electrode possesses superior cycling stability. For comparison, the V0-C electrode showed a decrease in capacity from the initial 200 mAh g^{-1} to only 102 mAh g^{-1} after cycling 500 times at the same current density, and the V-O-C electrode exhibited improved cycling performance compared with V0-C electrode, achieving a capacity retention of around 71.4% form 245 mAh g^{-1} at first cycle to 175 mAh g^{-1} after a continuous cycling for 500 times, slightly lower than that of N doped V-O-C (80%), suggesting that V and N co-doping also improved the cycling stability.

After the galvanostatic discharge/charge cycling tests at a current density of 6.4 A g^{-1} for 500 cycles, the half-cell was disassembled and the film electrodes were subjected to SEM examination. As shown in **Fig. 6**, the nanofiber morphologys were well maintained after the cycling, suggesting the good flexibility of the nonwoven film electrodes. Compared with the fresh electrode shown in **Fig. 1b**, the surface of the nanofibers became considerably rougher, which was attributed to the SEI formation. It is known that a SEI is easily formed over an electrode material when discharging to a low potential (0.01 V in this study). Here, we used the conventional 1 M LiPF$_6$ as a liquid electrolyte, and the adoption of a more stable electrolyte, such as an ionic liquid, could largely avoid such SEI film formation, contributing to a further improved cycling lifetime.

Conclusions

We have successfully prepared a flexible nonwoven film composed of N and V co-modified amorphous carbon nanofibers (N doped V-O-C) by electrospinning using a V-containing organic solution precursor followed by a two-step calcination in argon and in a NH$_3$ atmosphere as a free-standing flexible film anode for LIBs. With the outstanding performance of the N doped V-O-C nanofiber film electrode, the capacity reached 1380 mAh g^{-1} at a current density of 0.1 A g^{-1}. Furthermore, for the first galvanostatic charge/discharge cycle, the Coulombic efficiency was as high as 63.3%. Compared with the similar nonwoven film composed of N and N-free (V0-C) carbon, the current N doped V-O-C nanofibers showed considerably improved capacity and cycling stability. After 500 galvanostatic charge/discharge cycles at a current density of 6.4 A g^{-1}, the N doped V-O-C film electrode retained a stable reversible capacity of approximately 200 mAh g^{-1}.

Acknowledgements

Notes and references

^{a}State Key Laboratory of Materials-Oriented Chemical Engineering. Fax: +86 25 83172242; Tel: +86 25 83172256; E-mail: shaozp@njtech.edu.cn, ^{b}College of Chemistry & Chemical Engineering. ^{c}Department of Chemical Engineering, Curtin University, Perth WA 6458, Australia ^{d}College of Energy, Nanjing Tech of University, No. 5 Xin Mofan Road, Nanjing 210009, China

1   Y. Nishi, J. Power Sources, 2001, 100, 101-106.
2   Y. Sha, B. Zhao, R. Ran, R. Cai and Z. Shao, J. Mater. Chem. A, 2013, 1, 13233-13243.
3   B. Scrosati and J. Garche, J. Power Sources, 2010, 195, 2419-2430.
4   J. Wang, Y. Zhou, Z. Shao, Electrochim. Acta, 2013, 97, 386 - 392.
5   B. Zhao, R. Cai, S. Jiang, Y. Sha and Z. Shao, Electrochim. Acta, 2012, 85, 636-643.
6   Y. Hu, X. Li, J. Wang, R. Li and X. Sun, J. Power Sources, 2013, 237, 41-46.
7   L. Ji and X. Zhang, Electrochem. Commun., 2009, 11, 795-798.
8   P. Zhang, J. Qiu, Z. Zheng, G. Liu, M. Ling, W. Martens, H. Wang, H. Zhao and S. Zhang, Electrochim. Acta, 2013, 104, 41-47.
9   X. Li, J. Liu, Y. Zhang, Y. Li, H. Liu, X. Meng, J. Yang, D. Geng, D. Wang, R. Li and X. Sun, J. Power Sources, 2012, 197, 238-245.
10   X. Li, D. Geng, Y. Zhang, X. Meng, R. Li and X. Sun, Electrochem. Commun., 2011, 13, 822-825.
11   X. Chen, B. Zhao, Y. Cai, M. O. Tadé and Z. Shao, Nanoscale, 2013, 5, 12589-12597.
12   J.R. Shi, X. Shi, Z. Sun, E. Liu, B.K. Tay, S.P. Lau. Thin Solid Films, 2000, 366, 169-174.
13   J.R. Shi, X. Shi, Z. Sun, S.P. Lau, B.K. Tay, H.S. Tan. Diamond and related materials, 2001, 10, 76-81.
14   J. Yan, B.-J. Xia, Y.-C. Su, X.-Z. Zhou, J. Zhang and X.-G. Zhang, Electrochim. Acta, 2008, 53, 7069-7078.
15   N. Kuwata, J. Kawamura, K. Toribami, T. Hattori and N. Sata, Electrochem. Commun., 2004, 6, 417-421.
16   L. Qie, W. M. Chen, Z. H. Wang, Q. G. Shao, X. Li, L. X. Yuan, X. L. Hu, W. X. Zhang and Y. H. Huang, Adv. Mater., 2012, 24, 2047-2050.
17   C. Kim, K. S. Yang, M. Kojima, K. Yoshida, Y. J. Kim, Y. A. Kim and M. Endo, Adv. Funct. Mater., 2006, 16, 2393-2397.
18   Y. P. Wu, E. Rahm and R. Holze, J. Power Sources, 2003, 114, 228-236.
19   M. Ishikawa, T. Sugimoto, M. Kikuta, E. Ishiko and M. Kono, J. Power Sources, 2006, 162, 658-662.
20   V. Subramanian, H. Zhu, and B. Wei, J. Phys. Chem., 2006, 110, 7178-7183.